Implementing Deep Learning for COVID-19 Segmentation within Low-Radiation CT Scans

Aayush Goradia
Duke University
aayush.goradia@duke.edu

Nathan Parikh
Duke University
nathan.parikh@duke.edu

Jason Stranne
Duke University
jason.stranne@duke.edu

Abstract

The abstract paragraph should be indented ½ inch (3 picas) on both the left- and right-hand margins. Use 10 point type, with a vertical spacing (leading) of 11 points. The word **Abstract** must be centered, bold, and in point size 12. Two line spaces precede the abstract. The abstract must be limited to one paragraph.

1 Introduction

2 Related Work

-find a covid analysis paper -look into the facebook imaging challenge for faster ct scans -go through the ppt roarke used ans see if there are any relevant papers

One final area of related work deals with studies that have been conducted to evaluate the performance of different loss functions with semantic segmentation. Specifically, segmentation problems with unbalanced classes are of particular interest. For most of the images, the segmented Covid-19 mask only makes up a fraction of the CT scan. It has been observed that the focal loss and the dice loss perform well in cases of unbalanced classes [1].

3 Methods

3.1 Data and Pre-processing

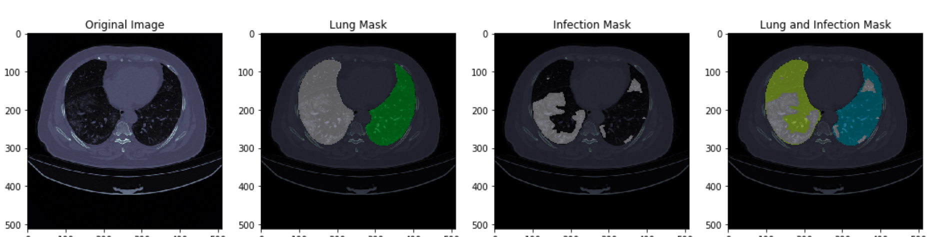

Figure 1: Examples of the images and mask labels that were provided in the data set

3.2 Physical Layer

3.3 CNN Architectures

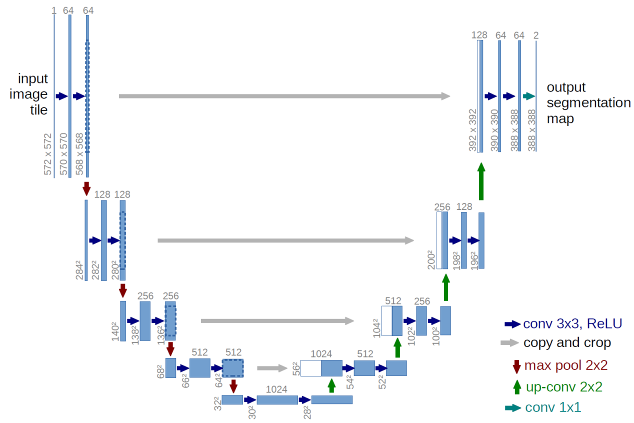

Figure 2: Visual representation of the U-Net architecture

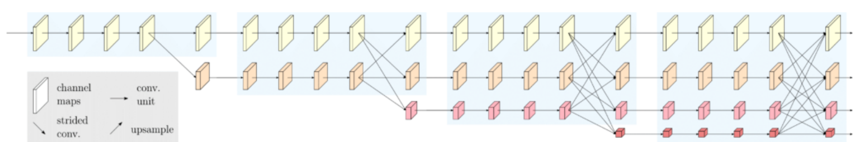

Figure 3: Visual representation of the HRNet architecture

3.4 Metrics

3.5 Training

$$-\alpha[y_i \times log(\hat{y}_i) + (1 - y_i) \times log(1 - \hat{y}_i)] - 2(\frac{y_i \times \hat{y}_i}{y_i + \hat{y}_i})$$

4 Results

5 Discussion

5.1 Future Work

Acknowledgments

We would like to thank Dr. Roarke Horstmeyer and Colin Cooke for their guidance in the planning and execution of this project.

References

[1] Shruti Jadon. A survey of loss functions for semantic segmentation. *arXiv:2006.14822 [cs, eess]*, September 2020. arXiv: 2006.14822.

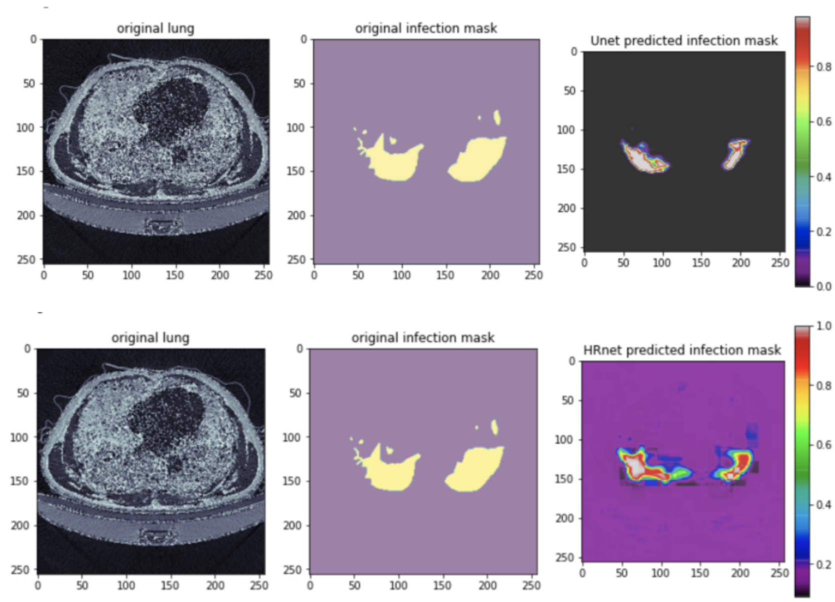

Figure 4: The predicted infection masks for both U-Net and HR-Net on the unmodified data set. HR-Net has a wider mask while U-Net predicts values closer to the binary extremes, 0 and 1.

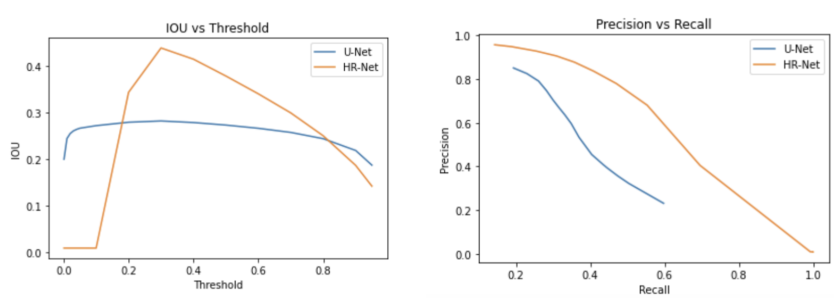

Figure 5: The IOU vs Threshold (left) and Precision vs Recall (right) plots for U-Net and HR-Net on the unmodified data set.

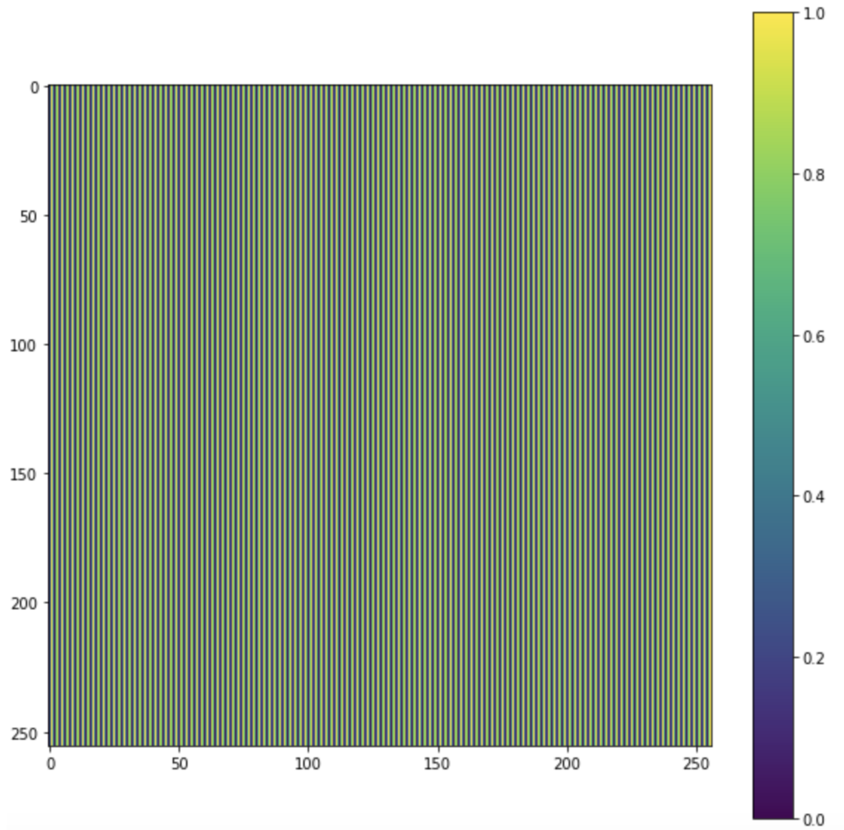

Figure 6: HR-Net Fourier Transform column weights for optimized physical layer with HR-Net.

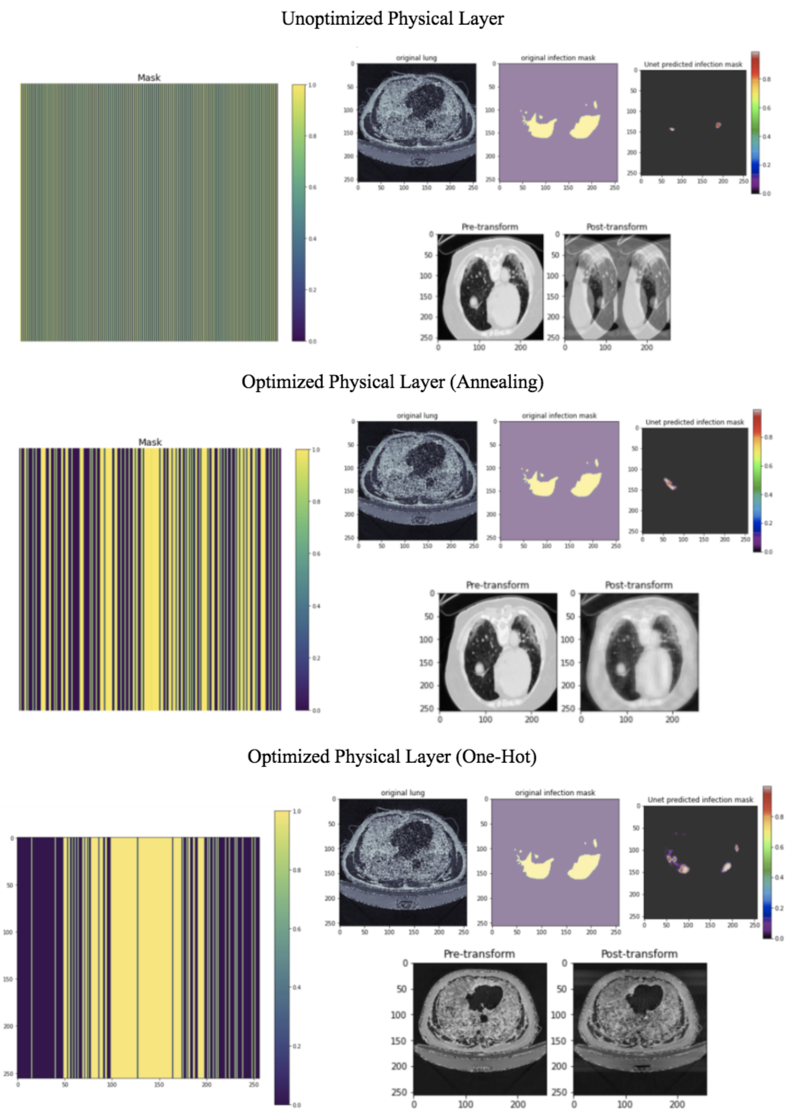

Figure 7: The mask (left), mask predictions (upper right), and transformed images (lower right) are shown for the unoptimized, annealing-optimized, and One-Hot-optimized scenarios.

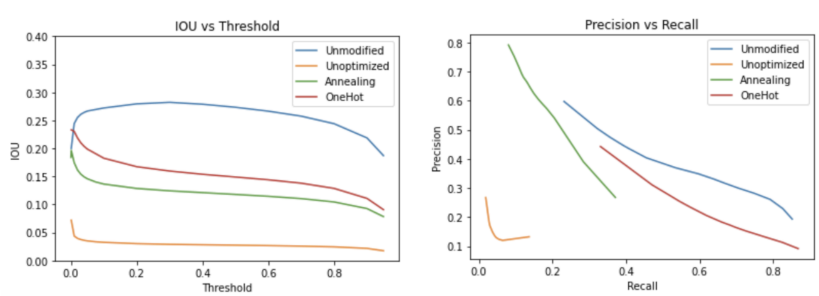

Figure 8: The precision-recall (left) and IOU plots for the unmodified data set, unoptimized physical layer, annealing, OneHot scenarios.

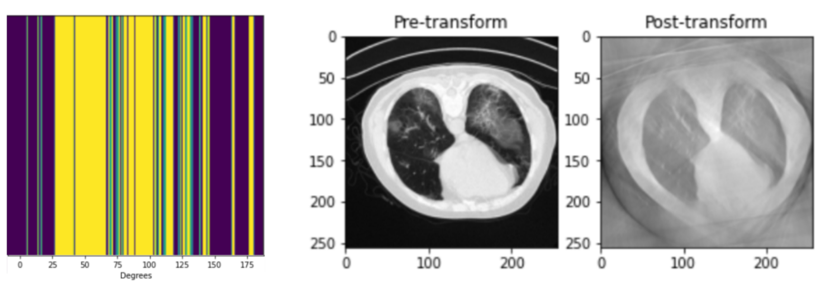

Figure 9: Learned radon transfer mask (left) and sample physical layer transformation using the experimental projection selection.